Marine Chemistry 187 (2016) 35–42

Contents lists available at ScienceDirect

Marine Chemistry

journal homepage: www.elsevier.com/locate/marchem

Precipitation/dissolution of marine evaporites as determinants in groundwater chemistry in a salt marsh (Península Valdés, Argentina)

María del Pilar Alvarez [a], Eleonora Carol [b,*], Pablo José Bouza [a]

[a] Instituto Patagónico para el Estudio de los Ecosistemas Continentales, (IPEEC-CENPAT-CONICET), Bv. Almirante Brown 2915, 9120 Puerto Madryn, Chubut, Argentina
[b] Centro de Investigaciones Geológicas (CIG-CONICET), Diagonal 113 Nro. 275, 1900 La Plata, Buenos Aires, Argentina

ARTICLE INFO

Article history:
Received 29 July 2016
Received in revised form 28 October 2016
Accepted 31 October 2016
Available online 2 November 2016

Keywords:
Geochemistry
Salt deposits
Coastal zones
Wetlands
Patagonia

ABSTRACT

Evaporites are mineral facies frequently occurring in salt marsh environments in arid climates. Considering that groundwater and soil salinity play an important role in the development of salt marsh ecosystems, the aims of this work are to study the occurrence and precipitation/dissolution processes of evaporites of marine origin and to evaluate how such processes influence groundwater chemistry in the Fracasso Beach salt marsh (Península Valdés, Argentina). Groundwater and seawater samples were collected for isotopic and chemical analysis. Ionic speciation and saturation indices were estimated, and the modelling of theoretical seawater evaporation was undertaken. The estimation of the isotopic variations due to evaporation was carried out according to an analytical model. To study the evaporites, soil salt crust samples were collected in the different sectors of the marsh and then observed in a scanning electron microscope with an X-ray energy-scattering micro-analyzer. The evaporite minerals occurring in different areas of the salt marsh show that there are changes in the dominance and type of evaporites depending on the topographic height. In the most elevated areas, abundant halite and gypsum/anhydrite precipitates are registered, accompanied by epsomite and bischofite, whereas in the lower salt marsh, mainly halite can be observed and, to a lesser extent, gypsum and scarce epsomite. The dissolution of all the evaporites is verified in the groundwater chemistry; the results show that the process of precipitation/dissolution of marine evaporites is the main determinant of groundwater salinity in the Fracasso Beach salt marsh. The variation in ion content registered within the salt marsh is related to the recurrence of the tidal flooding in each sector, as it renews the groundwater. This indicates that in the highest sectors the evaporation percentages are higher, and it confirms that the occurrence of evaporite minerals is determined by their closeness to the sea, the topographic height and, therefore, by the flooding frequency.

1. Introduction

In salt marsh environments of arid climates, evaporites are mineral facies frequently occurring (Butler, 1969). Most evaporite minerals found in such environments are the result of direct precipitation from the seawater that floods the salt marsh—mainly during spring high tides (syzygy) or storm events—which then evaporates (Warren, 2006). They may also form by the evaporation of subsurface seawater (Kinsman, 1976). Out of all the elements dissolved in seawater, only seven of them (Ca^{2+}, Mg^{2+}, Na^{+}, K^{+}, SO_4^{2-}, Cl^{-} and HCO_3^{-}) create stable and volumetrically significant salts as a product of seawater evaporation (Krumgalz and Millero, 1983; Hay et al., 2006; Butler et al., 2016). The experimental and empirical sequences of seawater evaporation were analyzed by mineral equilibrium (e.g., Eugster et al., 1980; Harvie and Weare, 1980); the HCO_3^{-} is not included, because it is consumed as calcite. In the Na-K-Mg-Cl-SO_4-H_2O system, the experimental sequence of seawater evaporation shows that, after gypsum ($CaSO_4 \cdot H_2O$) is converted to anhydrite ($CaSO_4$), halite (NaCl) precipitates. The next phase, that these authors determined under equilibrium conditions, is glauberite ($Na_2Ca(SO_4)_2$), which crystallizes at the expense of anhydrite. In this sequence, continued evaporation leads to glauberite resorption and eventual replacement by polyhalite. Finally appear the magnesium sulphates (probably epsomite $MgSO_4 \cdot 7H_2O$), which are joined by carnallite ($KMgCl_3 \cdot 6H_2O$). Although the relationships between the K^{2+}, Mg^{2+} and SO_4^{2-} ion activities during the evaporation process could lead to variations in the evaporite precipitation sequence, in general terms, the described sequence is the most representative.

As regards arid-region salt marshes, Schreiber and Tabakh (2000) indicate that the three main factors controlling the formation and accumulation of evaporites are the initial ion content, temperature and relative humidity. The present-day formation of evaporites in arid climate salt marshes (sabkhas) has been studied in the Arabian Gulf (Shearman, 1963; Butler, 1970; Kirkham, 1997), in the Gulf of Aqaba and the Red Sea (Attia, 2013; Aref et al., 2014), on the coast of the

* Corresponding author.
E-mail addresses: alvarez.maria@conicet.gov.ar (M.P. Alvarez), eleocarol@fcnym.unlp.edu.ar (E. Carol), bouza@cenpat.edu.ar (P.J. Bouza).

http://dx.doi.org/10.1016/j.marchem.2016.10.005
0304-4203/

Mediterranean (West, 1979), on the coast of Australia (Warren, 1982) and the coast of North Africa (Perthuisot, 1980).

In the littoral zone of Argentine Patagonia, salt marsh environments in arid and semi-arid conditions are numerous; however, few studies on evaporite formation have been undertaken. Many of the Patagonian salt marshes are natural reserves, where the formation of evaporite salts and the water chemistry affect the development of ecosystems (Isacch et al., 2010). Despite the fact that the ecology of tidal marsh plants mostly depends on a combination of multiple factors (Silvestri et al., 2005)—such as flooding frequency, soil salinity and saturated/unsaturated flow in the soil—for most species, salinity is the primary control on plant distribution (Watson and Byrne, 2009). In particular, salinity stress probably plays a much more important role in mediating plant zonation patterns at lower latitudes (PenningsS et al., 2005). The undertaking of detailed studies that would make it possible to understand what processes determine such characteristics is vital for the preservation of the environment. The objectives of this work are to study the occurrence and precipitation/dissolution processes of evaporites of marine origin in the Fracasso Beach salt marsh (Península Valdés) and to evaluate how such processes influence groundwater chemistry.

2. Study area

Fracasso Beach, located in Península Valdés (Fig. 1), consists of an open coast and a bay marsh (Bouza et al., 2008) with no inflow from permanent surface water courses. The tidal regime is semi-diurnal, with amplitudes of approximately 4 m at quadrature and up to 9 m at syzygy (Fig. 2). Its climate is characterized by an annual precipitation of 230 mm, with no definite trend throughout the year, and a mean annual temperature of 13.4 °C, fluctuating between mean extremes of 6.4 °C in July and 20.4 °C in January. The potential evapotranspiration, estimated for reference following Thornthwaite and Mather (1957), is 700 mm/yr with a water deficit every month.

The main geomorphological features of Fracasso Beach are a sandy tidal plain, the marsh and coalescing alluvial fans, known as bajadas (Fig. 1) (Alvarez et al., 2015a). The marsh is a low area with heights that do not exceed 8.5 m a.s.l. and a gentle slope, with a drainage that is generally deficient. The marsh shows vegetation zonation, characterized by *Spartina alterniflora*, in its lower part, and *Sarcocornia perennis* and *Spartina densiflora* in its upper part. In the tidal creek levees, which constitute relatively high areas, patches of *Limonium brasiliense* can be observed (Ríos et al., 2012; Idaszkin et al., 2014). In the areas where *Spartina alterniflora* dominates, heights do not exceed 6.5 m a.s.l. and they are flooded daily by the tides. In turn, in the upper part, heights vary between 7.8 and 8.5 m a.s.l. in the highest sectors, which are close to the upper edge of the salt marsh, where it borders with the bajadas. Regarding the flooding of the salt marsh, it mainly occurs during spring high tides and its reach and recurrence are mostly determined by the topography. The sectors whose height is below 7.5 m a.s.l. are flooded at every syzygy, and those with heights exceeding 8.0 m a.s.l. are only affected during new moon spring tides and extraordinary events (Alvarez et al., 2015b) (Fig. 2). The areas with soil salt crust development are associated with these locally high topographic sectors (i.e., the upper marsh near the bajadas and the tidal creek levees) (Fig. 1).

Concerning salt marsh groundwater, it receives the contribution from the bajadas and it discharges towards the tidal plain, defining a regional flow towards the sea (Fig. 1). However, the flooding caused by the tidal flow represents the main contribution to the water table. This infiltration causes a rise in the water table, accompanied by an increase in groundwater salinity (Fig. 2), which is attributed to the leaching of salts from the sediment (Alvarez et al., 2015b).

3. Methodology

Considering the geomorphological variations, the groundwater sampling points were located along three transects from the upper marsh

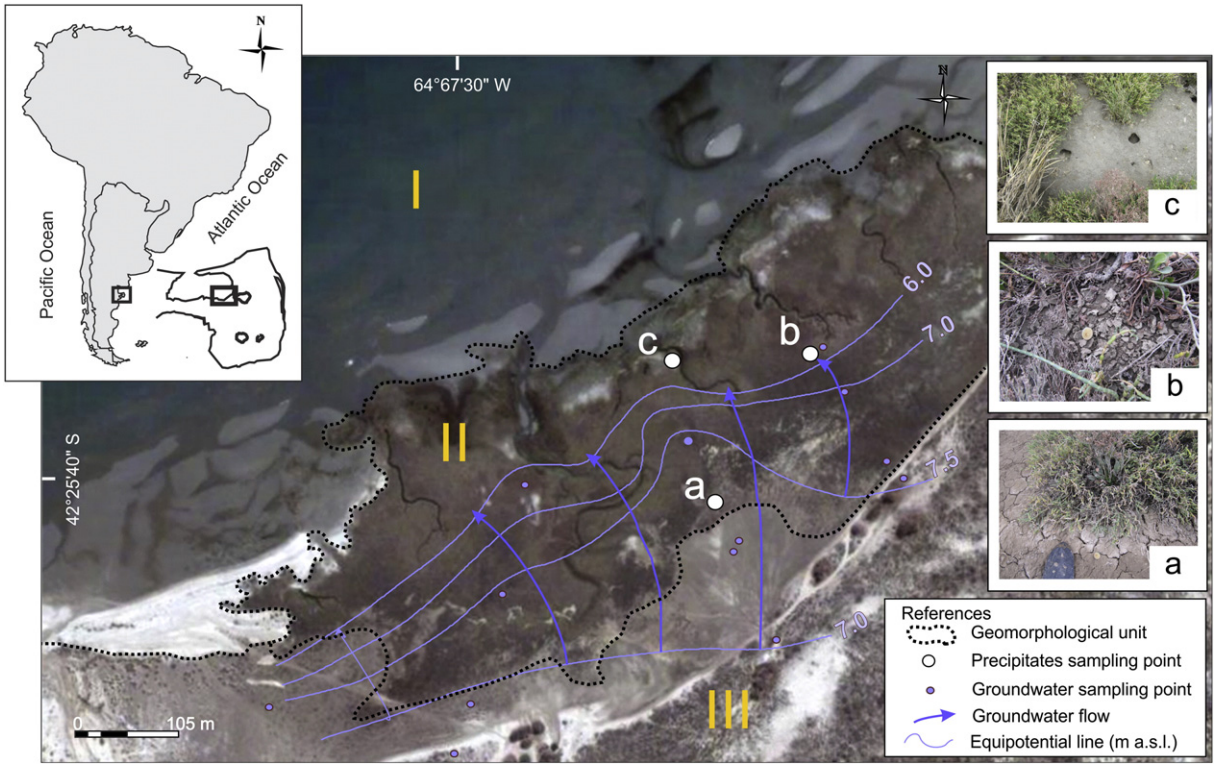

Fig. 1. Location map showing the monitoring network, the groundwater flow and the main geomorphological units: (I) Coastal Plain, (II) Marsh, (III) Coastal bajadas. The photographs on the right-hand side show the selected sampling points with their associated vegetation: (a) *Sarcocornia perennis*; (b) *Limonium brasiliense*, (c) *Sarcocornia perennis* and *Spartina densiflora*.

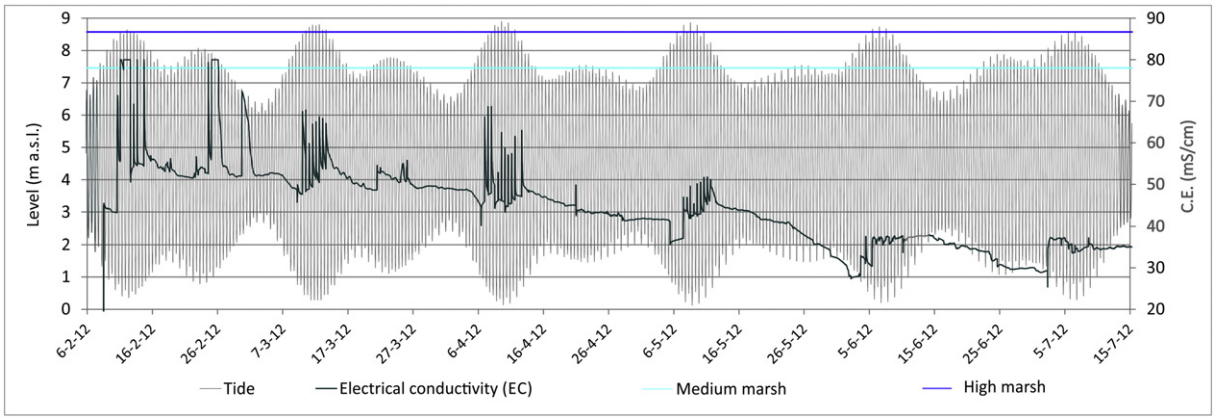

Fig. 2. Predicted tide for Fracasso Beach and electrical conductivity variations for a well in the upper limit of the marsh. In blue and light blue, topographic heights of the sampling points located in the lowest and highest sectors of the upper marsh.

towards the lower marsh. Eighteen samples of salt marsh groundwater from shallow boreholes (depths of up to 2.3 m) were collected, as well as sea water, for isotopic and chemical laboratory determinations. Besides, the piezometric levels were measured, always at low tide, throughout three sampling campaigns (April 2010, August 2011 and February 2012). At the same time, the pH, temperature and electrical conductivity were measured in the field with a multiparameter portable meter (Hanna HI 9828).

Groundwater and seawater sample collection, preservation and chemical analysis of major ions (Ca^{2+}, Mg^{2+}, Na^{+}, K^{+}, Cl^{-}, SO_4^{2-}, HCO_3^{-} and NO_3^{-}) were carried out in accordance with the standard methods proposed by the American Public Health Association (APHA, AWWA and WPCF, 1997). The charge balance error was below 5% for all samples (Table 1). Isotopic ratios $\delta^{18}O$ and $\delta^{2}H$ were measured by laser spectroscopy with equipment developed by Los Gatos Research (Lis et al., 2008). Results are reported following the usual convention δ (‰) vs. V-SMOW (Gonfiantini, 1978). Analytical uncertainties were ± 0.3‰ for ^{18}O and ± 1‰ for ^{2}H.

In order to assess water salinization in the salt marsh as a result of evaporation processes, an estimation of the isotopic variations due to evaporation was carried out according to the analytical model defined by Gonfiantini (1986), which is based on the approach by Craig and Gordon (1965). This model considers a drying-up water body, without inflow or outflow, and from which water is only removed by the evaporation process. Under these conditions, solute concentration can be expressed as a function of the evaporated water fraction. Thus, the enriched C' concentration can be estimated as:

$$C\prime = \frac{C_0}{(1-x)} \tag{1}$$

where C_0 is the initial concentration and x, the evaporated water fraction (i.e., $x = V / V_0$, with V being the present volume and V_0 the initial volume). Gonfiantini states that the isotopic water composition, δ, varies with the decrease in the remaining water volume fraction, $f = V / V_0$. Therefore the relationship between these two variables can be estimated as follows:

$$\frac{d\delta}{d\ln f} = \frac{h(\delta-\delta_\alpha)-(\delta+1)\left(\Delta\epsilon+\frac{\epsilon}{\alpha}\right)}{1-h+\Delta\epsilon} \tag{2}$$

where h is the relative humidity of the air; δ_α, the isotopic composition of the atmospheric water vapour; and α, the equilibrium fractionation factor ($\epsilon = \alpha - 1$). After an integration (δ_0 defined as the initial isotopic composition of water at $f = 1$), Gonfiantini's expression for δ (f) becomes:

$$\delta = \left(\delta_0 - \frac{A}{B}\right) f_B + \frac{A}{B} \tag{3}$$

Table 1
Physico-chemical data. TDS in µS/cm and concentration of major ions in mmol/L.

Sample	TDS	pH	HCO_3^-	SO_4^{-2}	Cl^-	Ca^{+2}	Mg^{+2}	Na^+	K^+	Error (%)	$\delta^{18}O$	$\delta^{2}H$
PF2.1	36,799	7.0	3.1	30.4	577.5	11.6	57.1	472.2	12.3	−1.54	−0.9	−7.0
PF2.2	35,884	7.1	2.5	28.8	557.7	11.1	54.1	478.7	10.2	0.12	−0.8	−4.0
PF2.3	41,219	6.7	3.2	34.1	633.8	12.5	63.2	553.5	12.7	0.87	0.2	0.2
PF4.1	56,768	6.8	5.1	41.9	903.4	21.2	81.6	734.8	16.5	−1.81	−1.4	−14.0
PF4.2	65,018	6.7	6.2	51.6	1009.0	23.3	96.7	867.8	16.3	0.25	−1.5	−14.0
PF4.3	73,812	6.7	7.7	59.8	1140.0	25.3	109.3	985.2	20.8	0.31	−0.3	−7.0
PF5.1	46,273	7.0	3.6	34.1	729.3	14.6	69.6	612.2	13.9	−0.42	−0.4	−4.0
PF5.2	35,824	7.7	2.4	28.2	569.6	11.1	55.0	458.3	11.1	−2.19	−0.3	−3.0
PF5.3	53,501	7.3	6.0	37.6	837.5	16.7	83.8	715.2	16.6	0.76	0.3	0.4
PF7.1	65,020	6.7	6.9	46.9	1016.3	24.0	88.4	881.7	16.5	0.26	−0.5	−5.0
PF7.2	57,639	7.0	5.8	41.8	931.5	18.8	85.5	728.7	16.0	−3.41	−0.2	−3.0
PF7.3	69,843	6.6	7.0	56.4	1056.9	23.6	110.5	957.4	21.8	2.91	0.4	0.7
PF11.1	16,738	7.4	5.1	17.9	239.2	7.0	15.9	232.6	4.3	0.46	−5.2	−42.0
PF11.2	30,191	7.3	5.2	26.8	464.5	8.2	42.1	395.7	9.3	−1.71	−3.6	−25.0
PF11.3	37,442	6.9	5.2	33.6	551.5	9.1	49.5	532.6	12.3	2.96	−3.9	−33.1
Sea.1	34,922	8.2	1.2	25.0	553.0	11.3	55.1	459.6	10.6	−0.08	−0.1	−3.0
Sea.2	34,237	8.2	1.7	27.8	541.1	10.7	54.5	438.3	10.4	−1.63	−0.3	−2.0
Sea.3	35,837	8.2	1.9	29.6	542.3	11.5	57.2	493.0	10.7	3.03	0.1	−0.7

where A and B are given by:

$$A = \frac{h\delta_\alpha + \Delta\epsilon + \epsilon/\alpha}{1-h+\Delta\epsilon} \quad (4)$$

$$B = \frac{h-\Delta\epsilon-\epsilon/\alpha}{1-h+\Delta\epsilon} \quad (5)$$

In order to do so, the initial concentration (C_0) was considered as the average of the seawater samples, with the relative humidity being on average 70%, value obtained from the Centro Nacional Patagónico (National Patagonian Centre, CENPAT) station, located in the city of Puerto Madryn (80 km to the southwest of the study area).

Then, to evaluate the possible mineral phases that could precipitate during seawater evaporation, a theoretical model was developed using PHREEQC 2.13 (Parkhurst and Appelo, 1999). In that model, the saturation indices were estimated for different seawater evaporation percentages, as shown in Eq. (6).

$$SI = \log\left(\frac{IP}{Kps}\right) \quad (6)$$

where *IP* is the ionic activity products and *Kps*, the solubility product constant, with the positive values showing oversaturation and the negative values, undersaturation.

In order to analyze the minerals of the soil salt crusts, representative samples of the marsh (Fig. 1) were collected, considering the high physiographic positions (i.e., high marsh near the bajadas, tidal creek levees and head of the tidal creeks (Fig. 1)). Of all the collected samples, the three most representative ones of each particular location were considered for the description. The sampling campaign was carried out a week after an extraordinary high tide that flooded the entire salt marsh, a condition that approximately occurs once a month, associated with the syzygies. The salt crust samples obtained have abundant detrital material, which makes it difficult to observe the evaporitic minerals with the electron microscope. For this reason, in the laboratory, the soil samples of less than 2 mm were crushed and saturation pastes were prepared with distilled water, and subsequently centrifuged at 9000 rpm for 40 min to extract the water with dissolved salts. The extract obtained was air-dried under laboratory ambient conditions on a microscope glass slide and the salt precipitates formed by evaporation were observed in a Jeol JSM 6460 LV scanning electron microscope with an EDAX PW7757/78 X-ray energy-scattering micro-analyzer (SEM-EDS), which was used to determine the qualitative composition of certain minerals.

4. Results

4.1. Hydrochemistry

The salinity of the seawater flooding the salt marsh fluctuates between 34,236 and 35,837 mg/L. The mean major ion contents are 552.9 mmol/L of Cl^-, 463.6 mmol/L of Na^+, 55.6 mmol/L of Mg^{2+}, 27.4 mmol/L of SO_4^{-2}, 11.2 mmol/L of Ca^{2+}, 10.6 mmol/L of K^+ and 1.6 mmol/L of HCO_3^- (Table 1). In turn, the groundwater samples from the salt marsh area have mean salinities of 48,131 mg/L, with maximum values higher than 70 mg/L in the summer, which progressively decrease towards the winter (Fig. 2). This higher salinity is reflected in an increase in the concentration of all the ions, which show mean values of 747 mmol/L of Cl^-, 640.4 mmol/L of Na^+, 70.8 mmol/L of Mg^{2+}, 37.9 mmol/L of SO_4^{2-}, 15.8 mmol/L of Ca^{2+}, 14.0 mmol/L of K^+ and 4.9 mmol/L of HCO_3^- (Table 1).

Taking into consideration the ions with higher concentrations (Cl^- and Na^+) and halite saturation, which is the main evaporite phase of such a pair, in the Na^+ vs. Cl^- plot it can be observed that groundwater shows an increase in these ions, with a tendency following that of the estimated seawater evaporation. This increase corresponds to evaporation percentages between 0 and 54%, leading to an increase in the halite saturation index (Fig. 3a and b). The Ca^{2+} vs. SO_4^{-2} ratio, as well as the gypsum saturation index vs. SO_4^{2-}, also shows that the content of these ions in the salt marsh groundwater samples increases following an evaporation trend with percentages between 0 and 54% as well (Fig. 3c and d).

Except for three samples—which were obtained near the recharge area of the bajadas and had $\delta^{18}O$ values between −5.2 and −3.6‰, and δ^2H values between −25 and −42‰ (Table 1)—the isotopic content of the salt marsh groundwater samples is similar to the mean value of seawater. These isotopic values are between −1.5 and 0.4‰ for $\delta^{18}O$ and between −2 and 1‰ for δ^2H. The relationships between isotopic content ($\delta^{18}O$) in terms of major ions show that the increase in all major ions occurs without isotopic enrichment (Fig. 4). This ion increase is 598 mmol/L for Cl^-, 492 mmol/L for Na^+, 53 mmol/L for Mg^{2+}, 30 mmol/L for SO_4^{2-}, 14 mmol/L for Ca^{2+}, 11 mmol/L for K^+ and 6 mmol/L for HCO_3^-. It should be noted that in these plots the salt marsh groundwater samples do not follow the estimated trend for seawater evaporation, registering in all cases an isotopic content that reflects very low evaporation percentages. The above-mentioned trend occurs in most samples, except for the three samples collected near the bajadas, which in general have lower major ion concentrations than seawater and depleted isotopic values.

4.2. Salt precipitates

The survey of salt precipitates carried out all over the salt marsh made it possible to identify areas with different levels of crust develop-

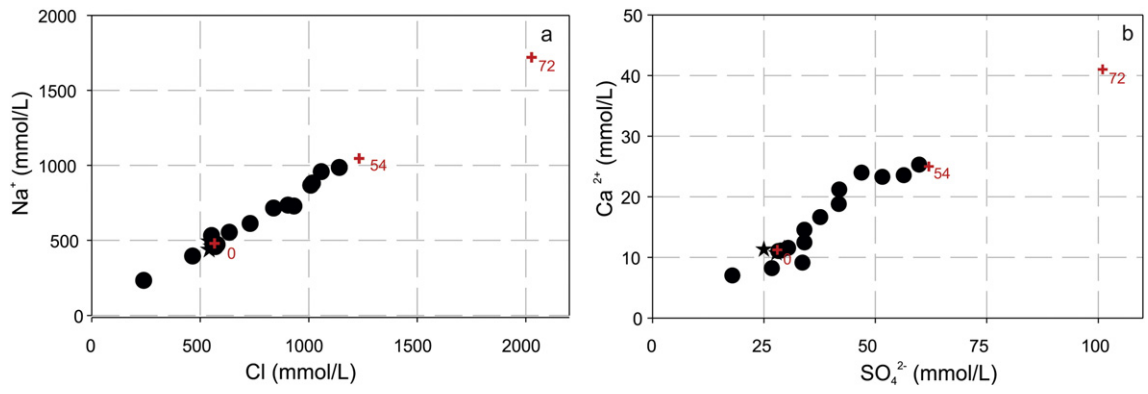

Fig. 3. Ion ratios and saturation indices. Red crosses indicate estimated evaporation percentages. Black dots plot salt marsh groundwater samples and black stars plot those of seawater.

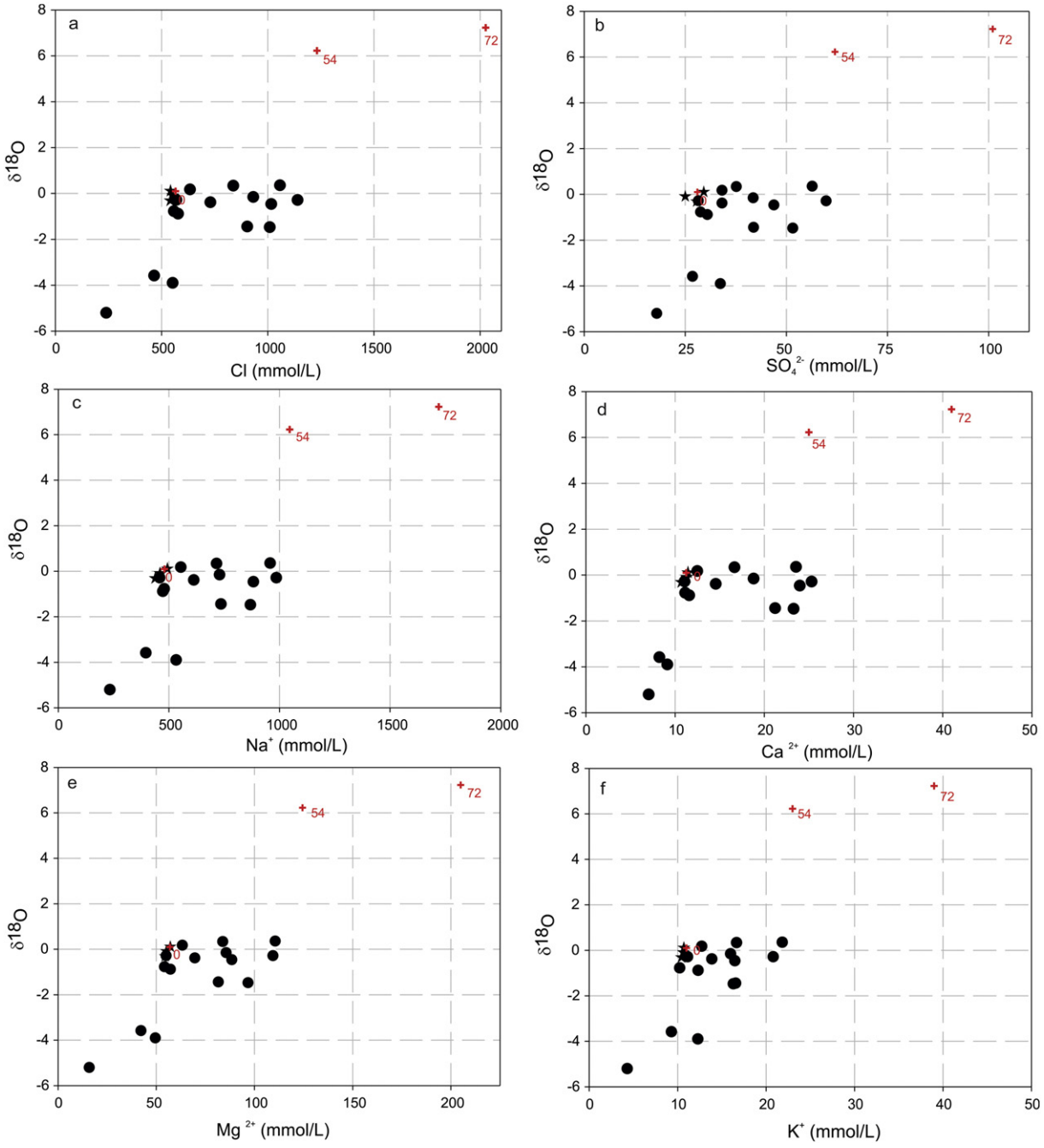

Fig. 4. ^{18}O vs. major ions. Red crosses indicate estimated evaporation percentages. Black dots plot salt marsh groundwater samples and black stars plot those of seawater.

ment. The sectors with better salt expression on the surface were identified on the upper edge of the salt marsh, almost on the border with the bajadas and on the banks of the tidal creeks. The salts obtained after the total desiccation of the saturation extracts were observed by SEM-EDS and they showed the dominance of halite and gypsum/anhydrite, and to a lesser extent of magnesium sulphate and magnesium chloride salts.

The abundance of the different mineral species in all the sampling sites is described and contrasted below, following a sequence from the sector located farthest from the sea towards the closest one, in order to observe whether there are variations depending on the topography, the flooding frequency and the associated vegetation.

The sector of the salt marsh farthest from the sea, whose height is about 8.5 m a.s.l., (site "a" in Fig. 1) is flooded by seawater with a recurrence that barely reaches 30 days (see tides and blue line in Fig. 2). In this sector, where the development of salt crusts was observed, the vegetation cover is low and, at the top of the soil profile, loamy–sandy sediments occur, underlain by sand.

The salt precipitates were identified on the basis of microscope images and their EDS spectrum, indicating the presence of abundant halite, which is recognizable due to its well-developed faces, perfect exfoliation and cubic habit. Besides, the EDS spectrum shows two well-defined peaks, one of Cl^- and another of Na^+, which validates its classification as NaCl. In second place, both in abundance and in the size of the crystals developed, comes gypsum, defined on the basis of its rosette habit and the twins observed (swallow tail twins), as well as its elemental pattern with well-defined peaks of S, O and Ca. In between crystals of halite

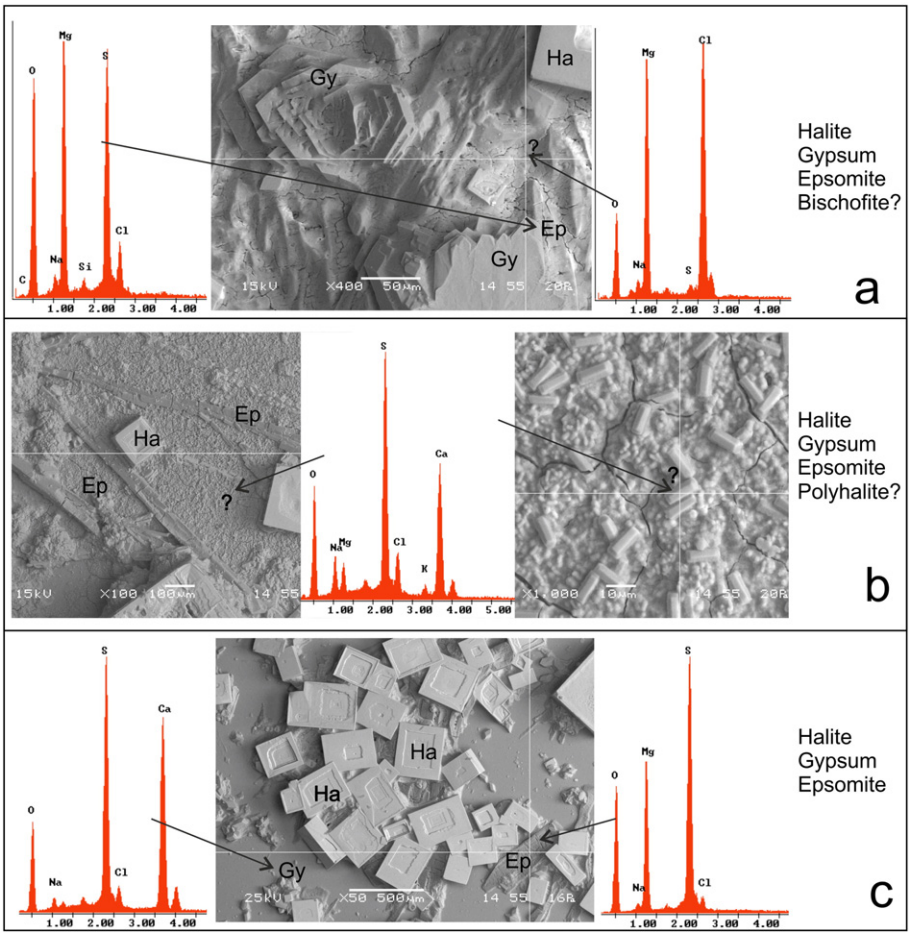

Fig. 5. Superficial salt deposits and mineralogy observed in an electron microscope from: (a) the upper marsh, (b) the tidal channel headwaters and (c) near the mouth of the tidal creeks (Gy: gypsum, Ha: halite, Ep: epsomite).

and gypsum, another less developed mineral with a fibrous habit occurs: its elemental composition suggests that it is a magnesium sulphate (Fig. 5a). Based on its morphology and mineral association, it may be said that it is epsomite ($MgSO_4 \cdot 7H_2O$). Finally, filling the spaces between epsomite crystals, there is an amorphous precipitate with an EDS spectrum showing two main peaks, one of Cl^- and another of Mg^{2+}, indicating that it is a magnesium chloride, possibly bischofite (Fig. 5a).

In the sites located on the banks of the middle to upper portions of the tidal creeks (site "b" in Fig. 1), whose height is about 7.8 m a.s.l., the soils are sandy loam, with an underlying sand layer. The minerals identified in a scanning electron microscope are halite, gypsum and epsomite, recognizable because they show the same habits and elemental peaks as those described for the previous sample. Much smaller in size, but occurring as a matrix to the larger crystals, a mineral of tabular habit was identified, with an EDS spectrum showing dominant peaks of S, O and Ca, and less defined peaks of Mg, Cl, Na and K (Fig. 5b). This possibly indicates that it is polyhalite ($K_2Ca_2Mg(SO_4)_4 \cdot 2H_2O$), as it is common in marine salt deposits, where it may constitute the major component; it is diagenetic in playa muds, and formed from gypsum in the presence of Mg–K-rich solutions (Anthony et al., 2016).

Continuing towards lower areas of the low salt marsh and closer to the sea, samples of salt precipitates were collected from a sector close to the mouth of one of the tidal creeks, with a topographic height of 7.3 m a.s.l. (site "c" in Fig. 1). In this site, soi is sandy and flooding occurs at every syzygy. The salt precipitates show abundant well-developed, cubic halite crystals and, to a lesser extent, gypsum with a rosette habit and epsomite. In all three cases, the elemental peaks confirmed the classification (Fig. 5c).

5. Discussion

The results analyzed suggest that such high groundwater salinity may be mainly due to processes of partial seawater evaporation before infiltrating or to the dissolution of salts present on the soil surface. However, the possibility that other processes, such as direct evaporation from the capillary fringe or plant transpiration, may contribute salts to a lesser extent should not be ruled out. If the dominant process is partial evaporation, the increase in ion content should occur simultaneously with isotopic enrichment. On the other hand, if such groundwater salinity is due to the dissolution of sediment salts, the increase in ion content should occur without isotopic changes (Peters and Coudrain-Ribstein, 1997).

The high major ion concentration in the salt marsh groundwater of Fracasso Beach (with ions being twice as many mmol/L with respect to seawater), as well as the ratios between them (Fig. 3), suggests that it could be due to seawater evaporation. If that were the case, the seawater that floods at high tide would evaporate up to 54% (Fig. 3) before infiltrating, and the salinities observed in groundwater would be the result of a concentration due to the partial evaporation of seawater. However, the lack of isotopic enrichment (Fig. 4) rules out this process, only leaving salt dissolution as the mechanism responsible for the high groundwater salinity.

Previous studies, based on groundwater dynamics, temperature and salinity response to the tide in the Fracasso marsh, show that groundwater salinity is mainly associated with the leaching of the soil salts that enter with the sea water that infiltrates during flooding events (Alvarez et al., 2015b). The origin of these dissolved salts may be associated with the total evaporation of seawater. If the seawater evaporation

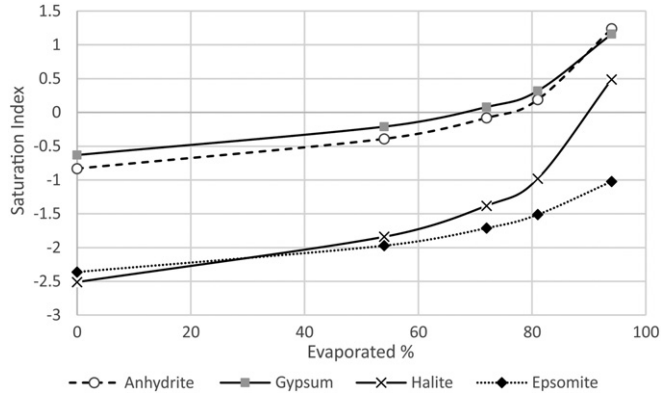

Fig. 6. Anhydrite, gypsum, halite and epsomite saturation index variations in relation to the percentage of evaporated seawater.

sequence in Fracasso Beach is considered, the results obtained when this process was modelled (Fig. 6) show that the calcium sulphate phases (gypsum and anhydrite) are the first ones to precipitate, with evaporation percentages close to 70%. Out of these two calcium sulphates, only gypsum was identified in the samples; however, the presence of anhydrite cannot be ruled out, as it is a very unstable evaporite due to its avidity for water. Halite saturation occurs when close to 90% of seawater evaporates. In the case of epsomite, even though its SI increases, it does not reach its saturation point, as the modelling was carried out up to an evaporation of 94% (Fig. 6), but it is to be expected for epsomite to form in a total evaporation sequence (Babel and Schreiber, 2014).

The study of the evaporite minerals occurring in different areas of the Fracasso Beach salt marsh shows that there are changes in the dominance and types of evaporites present depending on the topographic height (Fig. 5). In the most elevated areas, abundant gypsum, anhydrite and halite precipitates are registered, accompanied by epsomite and bischofite (Fig. 5a). The growth ratio observed between these minerals indicates the evaporation sequence. Gypsum and halite crystals are the first to form. Subsequently, it can be observed that epsomite precipitates between the gypsum and halite crystals, whereas bischofite precipitates between the epsomite crystals (Fig. 5a). The presence of these last two minerals indicates a high degree of evaporation, since they only begin to precipitate when the evaporation percentages exceed 98% (Warren, 2006). In the middle to upper portion of the tidal creeks, gypsum and halite precipitates continue to dominate, accompanied by epsomite and polyhalite, whereas in the lower salt marsh mainly halite can be observed, and to a lesser extent, gypsum and scarce epsomite.

The presence of bischofite in the most elevated sectors of the salt marsh and the decrease in the amounts of epsomite from the higher sector towards the lower sector show that in the most elevated sectors of the salt marsh the percentages of evaporation may be higher. Similarly, it can be considered that, in every sector under study, practically all of the seawater that flooded the salt marsh has evaporated (over 98%), a characteristic suggested by the presence of epsomite.

The results obtained are consistent with previous works that demonstrate that soil salinity in salt marshes increases with the topographic height, reaching its maximum value at a point coinciding with the highest high tide level, and then decreasing beyond this point (e.g., Adam, 1990; Silvestri et al., 2005). This is due to the fact that the highest sectors in the salt marsh, which are only flooded by certain spring high tides, have a longer time of exposure to evaporation.

The formation of evaporites on the surface of sediments is a frequent process in salt marshes in arid climates, where there is a deficit in the annual water balance (De Leeuw et al., 1991). As regards the presence of highly soluble evaporites—such as epsomite and bischofite—in the Fracasso Beach salt marsh, it is to be expected for their crystals to occur in metastable forms that may dissolve with the atmospheric humidity (Schreiber and Tabakh, 2000). Even though such evaporites may be stable in arid salt marshes, they are more typical of marine environments with high temperatures and evaporation rates, such as the areas of the Arabian Gulf, the Dead Sea or the Red Sea (Butler, 1969; El-Omla and Aboulela, 2012; Aref et al., 2014).

The dissolution of all the evaporites described can be verified in the groundwater chemistry (Fig. 4). The largest increases with respect to seawater are registered in the Na^+ and Cl^- ions, which are the result of halite dissolution, with halite being the most abundant evaporite. Sulphate evaporites contribute SO_4^{2-} anions and Ca^{2+} cationsin the case of gypsum–anhydrite, and Mg^{2+} in the case of epsomite. It should be noted that the increase in SO_4^{2-} reaches 60 meq/L, whereas the increases in Ca^{2+} and Mg^{2+} reach 27 meq/L and 125 meq/L, respectively. If for each equivalent of dissolved epsomite, similar equivalents of SO_4^{2-} and Mg^{2+} are contributed to the groundwater, the highest amount of Mg^{2+} registered shows that the ion contribution from the dissolution of bischofite is important. The contributions from bischofite can also be observed in the increase in Cl^- concentrations, which cannot be explained only by the dissolution of halite. When dissolving, halite contributes the same number of Na^+ and Cl^- equivalents to groundwater; however, the increase in Cl^- registered is higher, with bischofite being another source of this anion. To a lesser extent, K^+ is also contributed by evaporite dissolution, originating—according to the identifications carried out—from the dissolution of polyhalite.

Therefore, the results obtained show that the process of precipitation/dissolution of marine evaporites is the main determinant of groundwater salinity in the Fracasso Beach salt marsh. The variation in ion content registered within the salt marsh is related to the recurrence of the tidal flooding in each sector, as it renews the groundwater. It should be noted that in the case of the samples from the upper edge of the salt marsh, on the border with the bajadas, groundwater salinity is lower than that of seawater and, when compared to it, it is depleted in isotopes (Fig. 4). Even though a high salinity level is to be expected in that site due to the fact that tidal flooding is infrequent, a water mixing process with the least saline contribution from the bajadas occurs (Alvarez et al., 2015a).

6. Conclusion

The process of precipitation/dissolution of marine evaporites is the main determinant of groundwater salinity in the Fracasso Beach salt marsh, and it constitutes a cycle that is related to the tides. The salt marsh is flooded by the high tide, and part of the water infiltrates, while the one that remains on the surface evaporates completely, forming salt precipitates. The following high tide that floods the salt marsh washes out these evaporites, with the dissolved ions entering the groundwater. In this cycle, part of the seawater once again remains on the surface and it evaporates completely, forming precipitates that will be dissolved in the following high tide.

The presence of gypsum and halite, together with epsomite and bischofite, which are registered in the upper salt marsh, and the decrease in epsomite content towards the lower salt marsh indicate that in the highest sectors the evaporation percentages are higher. In this way, it is confirmed that soil salinity increases with ground elevation, with its maximum coinciding with the highest high tide level.

The occurrence of evaporite minerals formed by the mentioned cycle is determined by their closeness to the sea, the topographic height and, therefore, by the flooding frequency. Understanding the processes that regulate the spatial and temporal variation in water and soil salinity constitutes an essential tool for the management and preservation of these environments.

Acknowledgements

The authors are very indebted to the Agencia Nacional de Promoción Científica y Tecnológica (National Agency for Scientific and Technological

Promotion) and the Consejo Nacional de Investigaciones Científicas y Técnicas (National Council for Scientific and Technological Research) of Argentina for financially supporting this study by means of their grants, PICT 2013–2248 and PICT 2012–687.

References

Adam, P., 1990. Saltmarsh Ecology. Cambridge University Press, Cambridge.

Anthony, J., Bideaux, R.A., Bladh, K.W., Nichols, M., 2016. Handbook of Mineralogy. Mineralogical Society of America, Chantilly (VA 20151–1110, USA). http://www.handbookofmineralogy.org/.

Alvarez, M.P., Dapeña, C., Bouza, P.J., Ríos, I., Hernández, M.A., 2015a. Groundwater salinization in arid coastal wetlands: a study case from Playa Fracasso, Patagonia, Argentina. Environ. Earth Sci. 73, 7983–7994.

Alvarez, M.P., Carol, E., Hernandez, M.A., Bouza, P.J., 2015b. Groundwater dynamic, temperature and salinity response to the tide in Patagonian marshes: observations on a coastal wetland in San Jose Gulf, Argentina. J. S. Am. Earth Sci. 62, 1–11.

APHA, AWWA, WPCF, 1997. Standard Methods for the Examination of Water and Waste Water. 19th ed. (Washington).

Aref, M.A., Basyoni, M.H., Bachmann, G.H., 2014. Microbial and physical sedimentary structures in modern evaporitic coastal environments of Saudi Arabia and Egypt. Facies 60, 371–388.

Attia, O.E.A., 2013. Sedimentological characteristics and geochemical evolution of Nabq sabkha, Gulf of Aqaba, Sinai, Egypt. Arab. J. Geosci. 6, 2045–2059.

Babel, M., Schreiber, B.C., Holland, H., 2014. Geochemistry of evaporites and evolution of seawater. In: Turekian, K. (Ed.), Treatise on Geochemistry, second ed. Elsevier, Oxford (9144 p).

Bouza, P.J., Sain, C., Bortolus, A., Ríos, I., Idaszkin, Y., Cortés, E., 2008. Geomorfología y características morfológicas y fisicoquímicas de suelos hidromórficos de marismas patagónicas. XXI Congreso Argentino de la Ciencia del Suelo, San Luis (CD-ROM edition).

Butler, G.P., 1969. Modern evaporite deposition and geochemistry of coexisting brines, the sabkha, Trucial Coast, Arabian Gulf. J. Sediment. Res. 39, 70–89.

Butler, G.P., 1970. Holocene gypsum and anhydrite of the Abu Dhabi sabkha. Trucial coast: an alternative explanation of origin. In: Rau, J.L., Dellwig, L.F. (Eds.), Third Symposium on the Salt 1. Northern Ohio Geological Society, Cleveland, OH, pp. 120–152.

Butler, B.M., Papadimitriou, S., Kennedy, H., 2016. The effect of mirabilite precipitation on the absolute and practical salinities of sea ice brines. Mar. Chem. 184, 21–31.

Craig, H., Gordon, L.I., 1965. Deuterium and oxygen variations in the ocean and the marine atmosphere. In: Tongiorgi, E. (Ed.), Stable Isotopes in Oceanographic Studies and Paleo-Temperatures, pp. 9–130 (CNR Lab. Geol. Nucl., Pisa).

De Leeuw, J., Van den Dool, A., De Munck, W., Nieuwenhuize, J., Beeftink, W.G., 1991. Factors influencing the soil salinity regime along an intertidal gradient. Estuar. Coast. Shelf Sci. 32, 87–97.

El-Omla, M.M., Aboulela, H.A., 2012. Environmental and mineralogical studies of the sabkhas soil at Ismailia—Suez roadbed, southern of Suez Canal district, Egypt. Open J. Geol. 2, 165–181.

Eugster, H.P., Harvie, C.E., Weare, J.H., 1980. Mineral equilibra in a six-component seawater system, Na-K-Mg-Ca-Cl-H_2O, at 25°. Geochim. Cosmochim. Acta 44, 1335–1347.

Gonfiantini, R., 1978. Standard for stable isotope measurements in natural compounds. Nature 271–534.

Gonfiantini, R., 1986. Environmental isotopes in lake studies. In: Fritz, P., Fontes, J.C. (Eds.), Handbook of Environmental Isotope Geochemistry. Elsevier, pp. 113–168.

Harvie, C.E., Wheare, J.H., 1980. The prediction of mineral solubilities in natural waters: The Na-K-Mg-CaCl-S04-H20 systems from zero to high concentration at 25°C. Geochim. Cosmochim. Acta 44, 981–997.

Hay, W.H., Migdisov, A., Balukhovsky, A.N., Wold, C.N., Flögel, S., Söding, E., 2006. Evaporites and the salinity of the ocean during the Phanerozoic: implications for climate, ocean circulation and life. Palaeogeogr. Palaeoclimatol. Palaeoecol. 240, 3–46.

Idaszkin, Y.L., Bortolus, A., Bouza, P.J., 2014. Flooding effect on the distribution of native austral Cordgrass Spartina densiflora in Patagonian salt marshes. J. Coast. Res. 30, 59–62.

Isacch, J., Escapa, M., Fanjul, E., Iribarne, O., 2010. Valoración ecológica de bienes y servicios ecosistémicos en marismas del Atlántico Sudoccidental. In: Laterra, P., Jobbágy, E.G., Paruelo, J.M. (Eds.), Valoración de servicios ecosistémicos: conceptos, herramientas y aplicaciones para el ordenamiento territorial. INTA, Buenos Aires (740 p).

Kinsman, D.J., 1976. Evaporites: relative humidity control of primary mineral facies. J. Sediment. Res. 46, 273–279.

Kirkham, A., 1997. Shorline evolution Aeolian deflation and anhydrite distribution of the Holocene, Abu Dhabi. Geoarabia 2, 403–416.

Krumgalz, B.S., Millero, F., 1983. Physico-chemical study of dead sea waters. III. On gypsum saturation in Dead Sea waters and their mixtures with Mediterranean Sea water. Mar. Chem. 13, 127–139.

Lis, G., Wassenaar, L.I., Hendry, M.J., 2008. High-precision laser spectroscopy D/H and 18O/16O measurements of microliter natural water samples. Anal. Chem. 80, 287.

Parkhurst, D.L., Appelo, C.A.J., 1999. User's guide to PHREEQC (version 2)—a computer program for speciation, batch-reaction, one-dimensional transport, and inverse geochemical calculations. U.S. Geological Survey Water-Resources Investigations Report. 99, pp. 4259–4312.

PenningsS, C., Grant, M.B., BertnessM, D., 2005. Plant zonation in low-latitude salt marshes: disentangling the roles of flooding, salinity and competition. J. Ecol. 93, 159–167.

Peters, N.E., Coudrain-Ribstein, A., 1997. Hydrochemistry. IAHS (Publication no. 244).

Perthuisot, J.P., 1980. Site etprocessus de la formation d'evaporitesdans la nature actuelle. Bull. Cent. Rech. Explor. Prod. Elf Aquitaine 4, 207–233.

Ríos, I., Bouza, P.J., Sain, C.L., Bortolus, A., Cortés, E.G., 2012. Caracterización y clasificación de los suelos de una marisma patagónica, NE del Chubut. XIX Congreso Latino Americano de Suelos and XXIII Congreso Argentino de la Ciencia del Suelo, Mar del Plata, Argentina 978-987-1829-11-8 (Extended abstract. CD-ROM).

Shearman, D.J., 1963. Recent anhydrite, dolomite and halite from the coastal flats of Arabian shore of the Persian Gulf. Proc. Geol. Soc. Lond. 1607, 63–65.

Schreiber, B.C., Tabakh, M.E., 2000. Deposition and early alteration of evaporites. Sedimentology 47, 215–238.

Silvestri, S., Defina, A., Marani, M., 2005. Tidal regime, salinity and salt marsh plant 427 zonation. Estuar. Coast. Shelf Sci. 62, 119–130.

Thornthwaite, C.W., Mather, J.R., 1957. Instructions and Tables for Computing Potential Evapotranspiration and Water Balance (Centerton).

Warren, J.K., 1982. The hydrological settings, occurrence and significance of gypsum in late Quaternary salt lakes in South Australia. Sedimentology 29, 609–627.

Warren, J.K., 2006. Evaporites: Sediments, Resources and Hydrocarbons. Springer (1036 p).

Watson, E.B., Byrne, R., 2009. Abundance and diversity of tidal marsh plants along the salinity gradient of the San Francisco Estuary: implications for global change ecology. Plant Ecol. 205, 113–128.

West, I.M., 1979. Primary gypsum nodules in a modern sabkha on the Mediterranean coast of Egypt. Geology 7, 354–358.